ISSN 1063-7710, Acoustical Physics, 2020, Vol. 66, No. 2, pp. 178–190. © Pleiades Publishing, Ltd., 2020.

OCEAN ACOUSTICS.
HYDROACOUSTICS

Dimension Reduction in Location Estimation—the Need for Variable Propagation Speed

J. L. Spiesberger*

Dept. Earth and Environmental Science, U. Pennsylvania, Philadelphia PA, 19104-6316 USA

**e-mail: johnsr@sas.upenn.edu*

Received March 3, 2019; revised September 17, 2019; accepted October 29, 2019

Abstract—Calling mammals, ships, and many other objects have been commonly located during the last century with two-dimensional (2D) models from measurements of a signal's Time Differences of Arrivals (TDOA) when the objects are not on the 2D surface. The overwhelmingly common method for locating signals with 2D models takes signal speed as constant and location is derived by intersecting hyperbolas. However, when correct locations are required for 2D models, the speed used to derive location must depend on the geodesic distance along the 2D model surface between the object and the instrument. For example, when this distance is zero, the speed needed for correct location must also be zero. The dimension reduction from three to two introduces large errors in 2D models both near and far from the instruments unless the variable speeds induced by the dimensional reduction are explicitly accounted for. In light of these findings, methods are derived for generating extremely reliable confidence intervals for estimated locations in 2D models and identifying regions of the 2D model where a 3D model is needed. Because speeds needed for correct location are spatially inhomogeneous in the extreme, isodiachrons emerge as a natural geometry for interpreting location instead of hyperbolas. These issues are caused by choice of coordinates, and the same phenomena occur when coordinate transformations are applied in other fields of physics.

Keywords: source localization, 2D location, TDOA, coordinate tranformation, reliable location, confidence interval, geometry, isodiachron

DOI: 10.1134/S1063771020020098

1. INTRODUCTION

Locations of a wide variety of objects and phenomena are often estimated with a two-dimensional (2D) model from measurements of the propagation times of signals. The objects and signal-measuring instruments are almost never on the 2D model's surface, e.g. a Euclidean plane. In other words, the location of the object is explicitly forced by the 2D model to reside on the 2D surface even though it is not there. There are tens of thousands of papers discussing these models dating to at least 1886 (p. 204 in [1]) and 1918 [2]). A Google search with "TDOA 2D location" yields 69 000 sites, where TDOA stands for Time Difference of Arrival. Modeling locations in 2D is ubiquitous. Contemporary examples include locating calling mammals in the ocean [3–6], sounds in a room via robots [7], ships [8], cell phones [9], lightning [10], wildlife radio transmitters [11], aircraft radio emissions [12], and theoretical developments [13]. These models derive locations by translating Time Difference of Arrival (TDOA) to difference of distance assuming signal speed is constant [3, 5, 7–13], the overwhelmingly-common case, or are constrained to a finite interval [4, 6], e.g. 1450...1500 m/s for the ocean. Over the last century, perhaps all authors missed a fundamental problem.

The problem is illuminated by requiring 2D models to yield correct locations in the absence of measurement errors. Calculation of the signal speed is needed for a correct location when the object is near a receiver but not on the 2D surface. Suppose an object has the same horizontal coordinate as this receiver but is 100 meters above. If the signal propagates at 1 m/s it arrives 100 s after emission. In the 2D model, the object is zero meters from the receiver, so the speed to use to get the object's horizontal location to equal the receiver's location is zero meters divided by 100 s: zero meters per second! Using the same simple idea, we see the speed needed to obtain a correct location must depend on the horizontal distance between the object and instrument when we remove the third spatial dimension from the location model. I cannot find any previous reference for this fact and is the raison d'etre for this study. In light of these simple findings, we quantify the regions of validity of 2D models, show how to extend their validity, provide a method for deriving extremely reliable confidence intervals for location, and explain how an unconventional geometrical shape naturally emerges as a means to derive

location. The topics are related to coordinate transformations in general, with similar behavior found in other applications (Sec. 7). To the best of my knowledge, most of the ideas in this paper are new. Since there are 69 000 web sites dealing with the topic of 2D models, it is difficult to identify novelty with certainty. I will point out findings I believe to be novel while respecting the possibility of previous discovery. The finding of zero speed is explainable with the simplest of mathematics but methods for obtaining reliable locations in 2D are not so simple. The variation of signal speed with horizontal distance from an instrument is purely due to the 2D model approximation. There is no analogous behavior when signals are explicitly located in three-dimensional (3D) space.

Scientists appear to feel more comfortable utilizing the 2D model when the objects are far from the instruments in the horizontal direction. But even so, these models are commonly used to locate signals even when the objects are near the instruments. For example, in 2017 scientists used recordings from bottom-mounted receivers at 40 m depth to locate whales near and far from their instruments (e.g. Fig. 2 in [6]). It is shown here the 2D model approximation can yield very large errors not only near the instruments but even *far* from the instruments, even when the vertical separation between the instruments and objects are tens of meters and the horizontal separations are many kilometers (Sec. 3). The 2D model approximation is, perhaps unintuitively, not valid even at large horizontal separations from the instruments.

It will be shown how to delineate regions on the 2D model-surface where the 2D approximation is valid and how to compute reliable confidence intervals in the valid regions. It is necessary to use 3D models in the non-valid regions. There are many ways of modeling locations in 3D, and the best choice is application-dependent. Li et al. [14] review 2D and 3D modeling with TDOA, Cummins and Murphy [15] review 2D and 3D models to locate lightning, Rascon and Meza review means to locate sounds with robots [16]. None of these papers notes the need to vary signal speed in 2D models due to the elimination of the third spatial dimension.

Reliable locations are important for at least two reasons. Firstly, we wish to understand the behavior of a vocalizing marine mammal in the presence of disturbing sounds such as air-guns or Navy sonars. Reliable locations are needed for censusing and understanding behavior. Secondly, we wish to track locations of sounds. If the model for location yields incorrect locations because the 2D approximation is invalid, the tracker is provided invalid data. Valid locations have a better chance of forming valid tracks.

It is natural to ask why 2D models are used when it is widely known they are approximations. Reasons include, objects are usually horizontally-far from the receivers and the 2D approximation seems like it should be valid, 3D models require too much computer time, 3D models are more complicated, 2D models are used ubiquitously, implying their validity, the receivers are all near the same vertical coordinate and cannot be used to estimate vertical coordinates of a source at similar vertical coordinates, and, lastly, we are happy with the object's horizontal location: there is no need for a 3D model.

The subject of this paper may seem disorienting to readers primarily familiar with 3D models. In the ocean and atmosphere, the speed of sound can vary vertically and horizontally by significant amounts. From this perspective, readers could wonder why any contemporary paper would discuss 2D models where speed is either constant, or, in a few cases, varies between specified bounds. For the reasons stated above, 2D models are commonly used. Understanding how to use them appropriately could be important.

We explain the problem from the perspective of planar 2D models, i.e. Flatland, (Sec. 2) and quantify errors when the 2D effective speed is constant (Sec. 3). The material in these two sections appears to be new. Errors can be eliminated when this speed's value varies with distance from each instrument. With these variations, location can be interpreted with an unconventional geometry (Sec. 4). The unconventional geometry is not new, but this appears to be the first publication to explain how its use eliminates errors from the 2D approximation. Sec. 5 explains how to incorporate the variable speed and the unconventional geometry in a model accounting for all significant phenomena effecting location in both the air and water. The model yields extremely reliable confidence intervals for location. Its reliability depends on accounting for the fact that the speed of the signal depends on coordinates, the signals propagate along one or more curved paths, there are errors in estimates of the TDOA, the 3D field of signal speed, and the coordinates of the receivers. It will be shown how to identify invalid regions of 2D models where 3D models must be used to obtain reliable locations. Showing how to identify valid and invalid regions appears to be new. The model in Sec. 5 has been tested with data and independently tested by others with success. Sec. 6 discuses other flatlands, namely spherical and spheroidal surfaces. This material appears to be new. Results are discussed in Sec. 7 and connections are made with other fields.

2. FLATLAND

2.1. Two- and Three-Dimensional Effective Speeds

Suppose it's desirable to model locations of objects emitting or reflecting signals. A signal propagates between points P1 and P2 in 3D space (Fig. 1). A measurement is made at P2. The signal propagates between the points following the laws of physics, not usually the line segment of length d, unless the speed of the signal is spatially homogeneous.

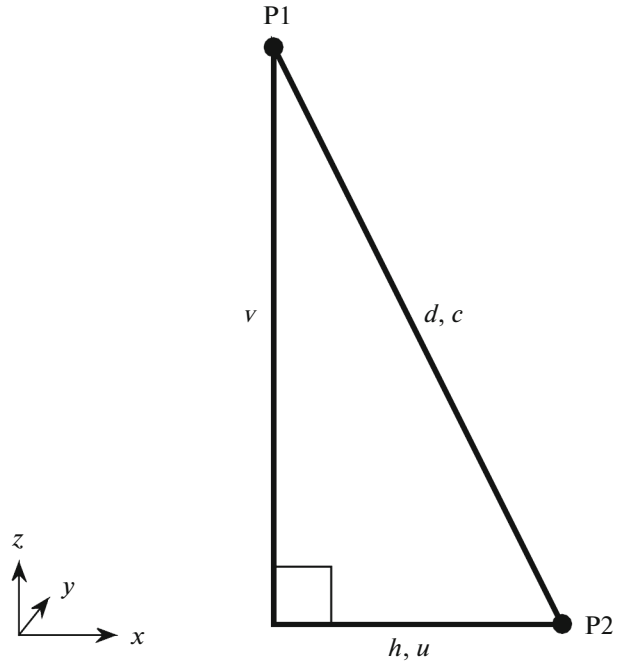

Fig. 1. Signal propagates between points P1 and P2. Distance of separation is d, with horizontal and vertical separations h and v. xy-plane is defined to be "horizontal" where locations are obtained from model. Both points may be out of xy-plane. Effective 3D and 2D speeds of signal are c and u respectively where horizontal separation h is parallel to xy-plane.

Define the 3D effective speed c to be the geodesic distance d between the points divided by the time t for the signal propagating between these points,

$$c \equiv \frac{d}{t}. \tag{1}$$

In flat space, the geodesic length is the Euclidean distance. The 2D effective speed u is adopted by the 2D model for location. It is defined to be the horizontal separation h between the points divided by the same propagation time t,

$$u \equiv \frac{h}{t}. \tag{2}$$

Solve Eq. (1) for t and substitute into Eq. (2) to get

$$u = \frac{hc}{d}. \tag{3}$$

2D and 3D effective speeds are identical when $h = d$: both points are on the 2D surface.

To see how the 2D effective speed depends on horizontal and vertical separation instead of horizontal and 3D separation, we use the Pythagorean relation $d = (v^2 + h^2)^{\frac{1}{2}}$ for d in Eq. (3),

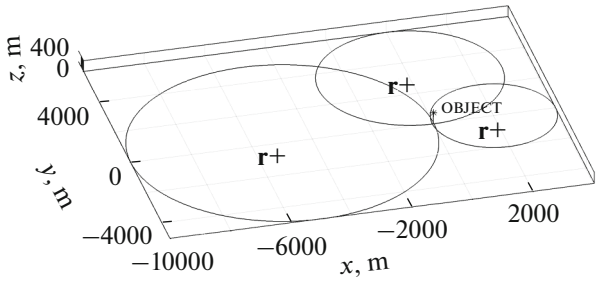

Fig. 2. Object (*) above Flatland. Each of three radars (r +) yield object's location on circle *in* Flatland since they know nothing of 3D space (Sec. 2.2). Circles intersect within 400 m of object's horizontal location (Fig. 3).

$$u = \frac{c}{\left(1 + \frac{v^2}{h^2}\right)^{\frac{1}{2}}}. \tag{4}$$

When either P1 or P2 are not on the 2D surface, v is not zero, and the 2D and 3D effective speeds differ. When the horizontal separation is zero and the vertical separation is not zero, the denominator in Eq. (4) goes to infinity and the effective speed is *zero*. Eq. (3) shows the same behavior: the length of the hypotenuse d exceeds the horizontal separation h, when the vertical separation is positive, so when h goes to zero, d remains positive and u goes to zero. The zeros of effective speed are problems for 2D models: they are caused by removal of the third spatial dimension.

2D and 3D effective speeds are not the same as another approximation called the "effective speed in a moving medium": the algebraic sum of the scalar speed of sound with the magnitude of the current or wind-vector.

2.2. Locating Signals in Flatland

The implication of estimating location in Flatland, a Euclidean plane, is explained assuming signal speed is a constant equal to 1450 m/s. In Flatland, nothing is known of 3D space. Flatland is the perspective of most papers utilizing 2D models, except the speed is set to some other constant whose value does not matter for the purposes illustrated here. A signal is transmitted to a receiver but its reception is weak. Scientists hypothesize an object in Flatland reflects the signal and arrives 180° out of phase with the direct path. To find the reflector, an acoustic "radar" is built. The distance to a reflecting object is obtained by measuring the round-trip travel time of the signal T. If time T_1 is measured it means the object is at distance $l_1 = cT_1/2$ where c is signal speed. The first measurement T_1 yields distance l_1, so the object is on a circle of radius l_1. The radar is moved, a second measurement is made wherein T_2 yields a distance l_2 whose corresponding circle intersects the first at two points. A third mea-

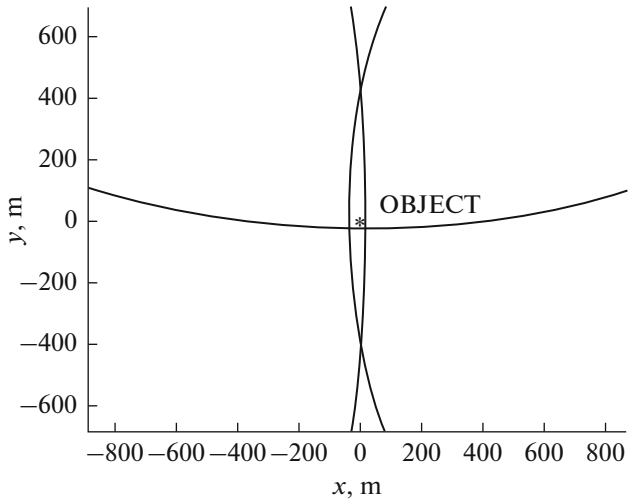

Fig. 3. Same as Fig. 2 except viewed above showing circles not intersecting at single point.

surement T_3 yields a third circle intersecting one point. Flatland scientists go to the hypothesized location and find the reflector. It is removed and signal reception is restored.

Sometime later, the reception disappears again. Scientists re-deploy their radar, unaware of the existence of an object in 3D space parked over Flatland with Flatland Cartesian location (0,0). Radars are deployed at three locations, and three circles are obtained whose points of intersection occur in the proximity of the origin (Fig. 2). From afar, the intersections look like a useful solution is obtained, but when the figure is enlarged the points of intersection differ by hundreds of meters (Fig. 3). Flatland scientists are unsatisfied because the accuracy of their measurements should yield a single location. Furthermore, they go to the area where the circles intersect but find no reflectors.

Because Flatland scientists cannot explain 400 m discrepancies in location, they move their radars close to the origin hoping for more accuracy, but instead obtain worse results (Fig. 4). In response, their theoretical physicists hypothesize the existence of a third spatial dimension of the universe, invent a new geometrical shape called a "sphere", use the same data to intersect three spheres, whose intersections occur at two points: their x-y origin and elevations $z = +-400$ m above and below Flatland. One of these is correct.

3. QUANTIFYING ERRORS WITH CONSTANT 2D EFFECTIVE SPEED

A common method for locating objects in 2D models is to assume the 2D effective speed is a constant. We quantify errors of this approximation, leaving discussion of other errors affecting location to Sec. 5.

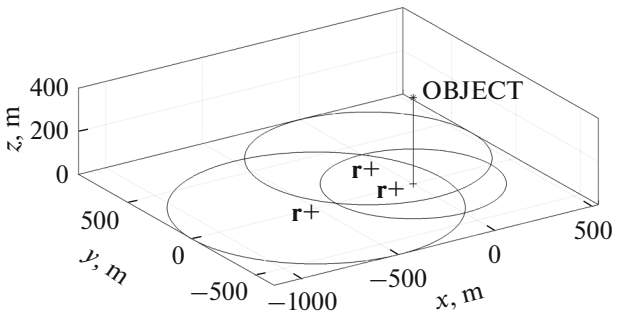

Fig. 4. Same as Fig. 2 except radars moved closer to the origin.

3.1. Direct-path Time

Suppose we estimate the time t for a signal to propagate between a source on Flatland and a reflector at perpendicular distance v from the surface. Flatland corresponds to $z = 0$ in Cartesian coordinates. Let the source be located at $x = 0$ and $y = 0$ (point P2, Fig. 1). The reflector is located at point P1 (x, y, $z = v$). In Flatland, the estimated distance to the reflector is

$$h_{\text{flat}} = c_{\text{flat}} t, \tag{5}$$

where c_{flat} is a constant. A constant value is the overwhelmingly popular method for locating signals with 2D models. The 3D distance to the signal is $d = ct$ where c is the 3D effective speed (Fig. 1). The projection of d onto Flatland is $h = \left(d^2 - v^2\right)^{\frac{1}{2}}$ or

$$h = d\left(1 - \frac{v^2}{d^2}\right)^{\frac{1}{2}}, \tag{6}$$

(Fig. 1). The error of the 2D location model is,

$$\epsilon \equiv h_{\text{flat}} - h = c_{\text{flat}} t - h = c_{\text{flat}} \frac{d}{c} - h. \tag{7}$$

Substituting Eq. (6) in Eq. (7), we get

$$\epsilon = \left[\frac{c_{\text{flat}}}{c} - \left(1 - \frac{v^2}{d^2}\right)^{\frac{1}{2}}\right] d. \tag{8}$$

A single speed is often adopted for the 2D model: the same as the 3D effective speed, $c_{\text{flat}} = c$. For direct-path times, this forces the error to zero when the reflector's horizontal distance is much greater than its vertical offset (Fig. 5a). Distances are normalized by vertical offset v because v is the geometrical parameter affecting error. Because errors are large when the horizontal offset h is small, we could choose a smaller value for c_{flat} yielding slightly smaller errors at small offsets and larger errors at large offsets (Fig. 5b). In the absence of knowledge of the source's horizontal and vertical location, it is impossible to know the correct value to choose for c_{flat} yielding zero error in location.

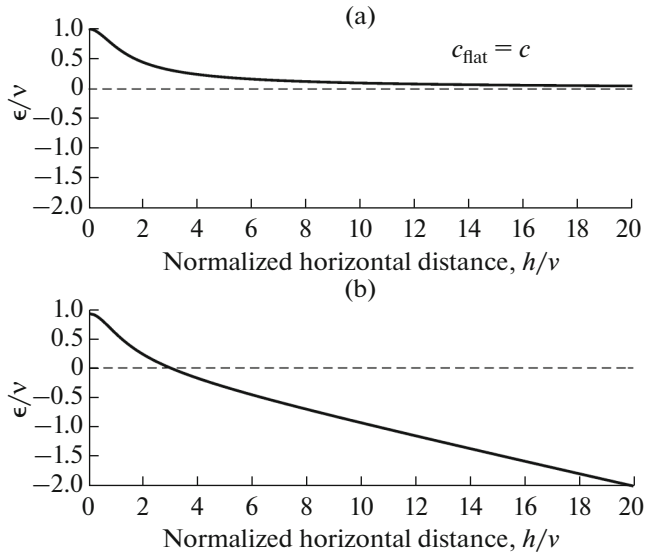

Fig. 5. (a) Error of 2D location model versus true horizontal location of 3D object when 2D model uses 3D effective signal speed c. Errors tabulated for locations derived from measurement of signal time between a source and receiver. Horizontal distance to object projected onto 2D model normalized by perpendicular distance v of object from 2D model (horizontal axis). Vertical axis is normalized error of 2D model ϵ/v, where ϵ is (Eq. 8). (b) Same except 2D model uses nine-tenths of 3D effective signal speed for purpose of slightly decreasing 2D model errors at smaller horizontal distances at expense of larger errors at large distances.

The purpose of showing Eq. (8) is to show errors in the 2D model as a function of the model's selection for signal speed.

3.2. Time Differences of Arrivals (TDOA)

We measure TDOAs from a source and estimate location with a 2D model. In some regions of the plane, three receivers are sufficient to yield a unique mathematical solution, yet other regions require four receivers [17]. Let the signal time between the source and receiver i be t_i. With R receivers, we measure TDOAs,

$$\tau_{ij} \equiv t_i - t_j, \quad i < j; \quad j = 2,3,\ldots R. \tag{9}$$

With three receivers, we measure τ_{12}, τ_{13}, and τ_{23}, but without errors of measurement τ_{23} provides no independent information since $\tau_{23} = -\tau_{12} + \tau_{13}$. Similarly, four receivers yields three independent TDOAs.

We adopt a single sound speed in the 2D model, c_{flat}. TDOAs are converted to a difference in distance from receivers 1 and j with

$$l_1 - l_j = c_{flat}\left(t_1 - t_j\right) = c_{flat}\tau_{1j}. \tag{10}$$

This is a hyperbola, the locus of points whose difference in distance is constant from two points. Location is obtained by intersecting hyperbolas. We set the 2D effective speed as c_{flat} = 1450 m/s: the same as the 3D effective speed. Consider a shallow-water scenario with source at 15 m depth and four receivers at 50 m depth. Four receivers are used to avoid the mathematical plurality of solutions with only three receivers [17]. We assume t_i =1, 2, 3, 4, are measured without error, yielding three independent TDOAs. Two hyperbolas are intersected, each derived from τ_{12} and τ_{13}. This yields the first set of intersected locations in the plane with 0, 1, 2, 3, or 4 points of intersection. If the source was in the plane of the model, a solution would always exist, but not necessarily when the source is out of the plane. If there are two or more points of intersection, a new hyperbola is formed from receivers one and four to attempt to resolve the ambiguity. The new hyperbola is intersected with the hyperbola from receivers one and two. These intersect at the second set of locations containing 0, 1, 2, 3, or 4 elements. If either the first or second set is empty, no solution for location is determined. If the first set contains two or more locations, and the second set is empty, we end up with ambiguous solutions. Otherwise we choose the single location from the first set whose distance is minimum to any of the locations from the second set. If the source was in the plane of the model, we would always have a single solution for location. The out-of-plane geometry introduces unavoidable complications as long as we insist on using a 2D model with a single speed c_{flat}.

Receivers are placed at horizontal Cartesian coordinates (−510, −500), (500, −490), (500, 507), and (−502, 506) m (Fig. 6). The source is placed at 200 m increments of x and y in an area 20 × 20 km^2 centered on the mean horizontal location of the receivers. The 2D model yields source locations (x_m, y_m). The error of each (x_m, y_m) is its distance to the true horizontal location. Unfortunately, very large errors occur at sub-grid intervals, so the plot greatly underestimates errors. It is impractical to search the horizontal space with enough resolution to reveal the largest error. For example, we decreased the grid interval from 200 to 0.2 m near receiver 1. The maximum error rose to several hundred meters. Then the grid interval was decreased to 0.1 m and the maximum error increased to 1781 m. The six ridges with large errors are caused by nearly-parallel asymptotes of the hyperbolas. Points of intersection of nearly-parallel asymptotes are sensitive to variation in 2D effective speed. Errors are tabulated in five distance intervals from the mean location of the receivers (Table 1). Mean errors are about 20 m. Maximum errors are large: between 600 and 1000 m. When the source is located within the x–y perimeter of the receiver's polygon, maximum error is at least 1781 m. Errors are large compared with the 35 m offset of the source from the model plane.

Next, the errors of this same problem are quantified when the 2D effective speed is 5 m/s less than the 3D effective speed of 1450 m/s (Fig. 6b). The asym-

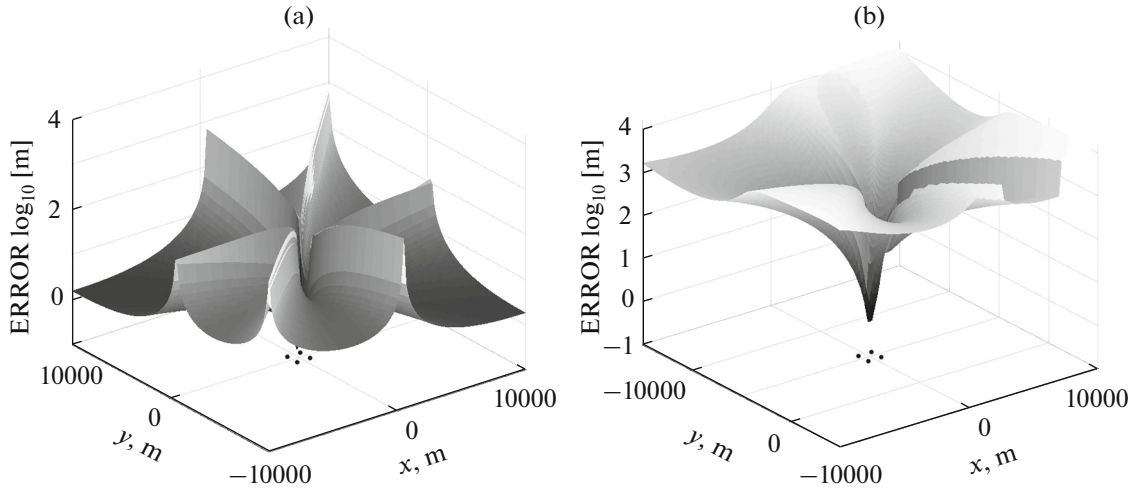

Fig. 6. (a) Maximum horizontal error of 2D (planar) location model derived with TDOAs from four receivers (dots) as function of horizontal location of acoustic source. Source and receivers at 15 and 50 m depth respectively. Vertical axis is $\log_{10}$ of error: two is 100 m. 2D effective speed equals 3D effective speed 1450 m/s. Errors due to non-coplanar objects and utilization of single 2D effective speed (Sec. 3.2). (b) Same as (a) except 2D effective speed is 5 m/s less.

metry in error with azimuthal angle is caused by the use of receiver one as the reference. The errors grow considerably with large values far from the ridges of Fig. 6a. The large errors are caused by the locations where the hyperbolas intersect (Fig. 7). When the errors grow to near 10000 m, the cause is due to the fact that the points of intersection are ambiguous, one set of points occurring near the receivers and the other set of points near a distant source. The two sets of points are separated by about 10000 m. Without further information about which cluster of intersections is correct, we are left with large errors. The importance of setting the 2D effective speed to equal the 3D effective speed correctly is important not only for direct-travel times (Fig. 5), but also for TDOA data. When TDOAs are derived from the arrival times of electromagnetic signals, it is easy to set the 2D effective speed to be the nominal speed of light. However, in the ocean and atmosphere, we usually do not know the 3D effective speed very accurately, which causes large errors in location.

3.3. Delineating Areas of 2D Models Where Errors are Acceptably Small

When objects are located with direct-path times, and when the 2D model's speed equals the 3D effective speed, correct locations are only obtained when the object's horizontal coordinates are infinitely far from the instruments (Fig. 5a and Eq. (8)). For locations derived from TDOA's, correct locations might be obtained at infinite distances in certain directions, but not in other directions where the errors grow with distance (ridges, Fig. 6a; plateaus Fig. 6b). Suppose we can accept location errors of the 2D model up to a maximum threshold equal to $\hat{E}$. This determines areas

Table 1. 2D model error in Fig. 6a due only to source being out of 2D model plane. 2D effective speed equals 3D effective speed. Distances computed with respect to mean horizontal location of receivers. Maximum horizontal distance of any receiver from mean is 716 m. Corresponding minimum, mean, and maximum errors in interval [0, 716] m are 0.14, 1.3, and at least 1781 m respectively. Errors are much larger when 2D effective speed is a little less than the 3D effective speed (Fig. 6b)

Distance interval, m	2D Model errors, m		
	minimum	mean	maximum
0 to 1999	0.14	15	≥1781
1999 to 3999	1	18	≥348
4000 to 5998	1	18	≥568
5998 to 7998	1	19	≥726
7999 to 9997	1	19	≥831

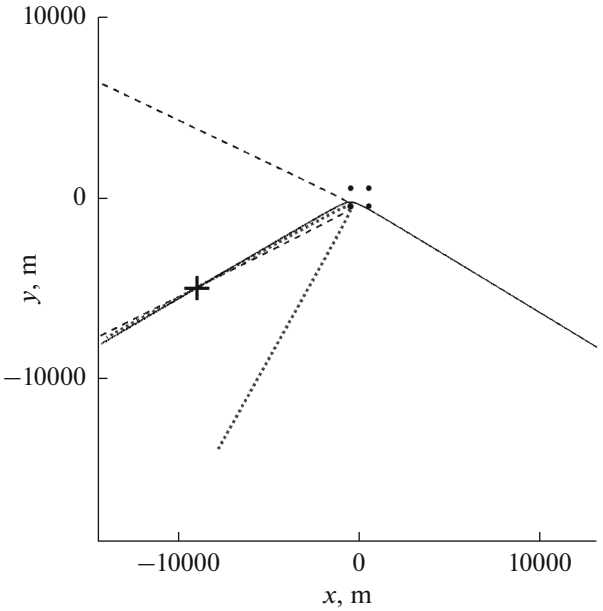

Fig. 7. Explanation for large errors in Fig. 6b. Four black dots in center are receivers. Location of source (+) estimated from intersection of three hyperbolas. Hyperbolas derived from receivers one through three intersect at two points, one very near the receivers and the other near the source. Hyperbola derived from receivers one and four also intersects the hyperbola from receivers one and two at two points, one near the receivers and one near the source. These points of intersection do not reveal if the location of the source is near the points of intersection far or near from the receivers.

of the 2D surface where acceptable errors are obtained. These areas are determined as follows. Errors of the 2D model $E(x, y)$ are computed via simulation as shown in Secs. 3.2 and 3.3. We receive I signal-time data, and compute their locations with the 2D model: (x_i, y_i), $i = 1, 2, 3, ...I$. We accept the i'th location when $E(x_i, y_i) \le \hat{E}$. Otherwise the datum is discarded. In this scenario, there remain holes in the 2D model where locations are not estimated because they have unacceptably large error.

3.4. Hybrid 2D and 3D Location Models

In Sec. 3, signals are located only when their 2D effective speeds have acceptably small error. Signal times are discarded when associated errors exceed the threshold. Instead of discarding these signals, we can estimate horizontal location with a 3D model, and use its 2D location. We have to pay the price for computing 3D locations for some but not all the data.

4. ELIMINATING ERRORS IN FLATLAND WITH VARIABLE 2D EFFECTIVE SPEED

The previous section quantified errors of location from 2D models when a single 2D effective speed is used to estimate location. If we do not wish the reduction of modeling dimension from three to two to contribute to location error, we must allow the signal speed to vary with horizontal separation from the instruments. When we include measurement errors, variation in signal speed must occur so as to obtain a reliable confidence interval for location.

Let us define the "valid regions" of a 2D model to be locations on the 2D surface where a correct location is obtained. When the 2D model accounts for errors in measurements, the valid regions are those for which a correct confidence interval for location is obtained without inflating errors contributing to uncertainty. For example, suppose the only measurement error is the estimate of the TDOA and its actual uncertainty is 0.01 s. Then if the confidence interval derived from the 2D model contains the object's true location at the specified confidence interval for location, the object is in a valid region of the 2D model. This definition of a valid region excludes the possibility of artificially inflating the uncertainty of the TDOA to obtain a reliable confidence interval of location.

Without loss of generality, we assume 2D locations are on a horizontal x–y plane and the object to be located has Cartesian coordinates (x, y, z). First, we explain how the 2D effective speed can be estimated from the data (Sec. 4.1). Then we explain how these estimates can be used to estimate location (Secs. 4.2, 4.3, and 4.4).

4.1. Effective Speed is Function of Measured Signal Time

The idea is to improve the accuracy of locating a signal by letting the 2D effective speed be a function of the measured signal time (s). Let $U(t, \boldsymbol{r}_j)$ approximate the 2D effective speed as a function of the measured signal time t and instrument location(s) $\mathbf{r}_j$. Explicit dependence of t on the object's location is implied but not shown. We think of $U(t, \mathbf{r}_j)$ as a single value, i.e. a 2D effective speed, or more generally a confidence interval of the 2D effective speed for each horizontal location in the model plane. A procedure for constructing $U(t, \mathbf{r}_j)$ is 1) specify locations of the instruments $\mathbf{r}_j$, 2) specify a 3D grid of hypothetical object locations (x_k, y_k, z_k), where the 2D effective speeds are computed at the instruments, 3) specify the 3D effective speed c, 4) use Eq. (4) to compute the 2D effective speed, $u(x_k, y_k, z_k)$, for each hypothetical object location in the grid, and 5) compute $U(t, \mathbf{r}_j)$ from $u(x_k, y_k, z_k)$. Here is an example. We want a 100% confidence interval for the 2D effective speed between instrument one and a fixed horizontal location $(x_k, y_k, z_k) = (X, Y)$ in the 2D model plane. Q values of k yield the same coordinate, (X, Y), but with different vertical coordinates, z_k. The minimum 2D effective speed at this point, $\check{u}$, is the minimum of $u(x_k, y_k, z_k)$ among all Q vertical coordinates

z_q; $q = 1, 2, 3, \ldots Q$. The maximum $\hat{u}$ is obtained similarly. The desired confidence interval is $U(t, \mathbf{r}_j) = [\check{u}, \hat{u}]$.

4.2. Direct-Path Times

For direct-path times, we receive a measurement of signal time, then use $U(t,\mathbf{r}_1)$ to obtain an estimate of the 2D effective speed. If we desire 100% confidence intervals for horizontal location, we compute $U(t,\mathbf{r}_j) = [\check{u}, \hat{u}]$, and draw the annulus about $\mathbf{r}_1$ whose inner and outer radii are $\check{u}t$ and $\hat{u}t$ respectively. The procedure is repeated for the signal time measured at a second instrument, yielding a second annulus. The object's horizontal location resides in the intersection of the two annuli: either one region or two non-overlapping regions. Data from a third instrument yields a third annulus whose intersection yields one or two contiguous regions of the plane. If we desire locations with less than 100% confidence, we repeat the procedure using p% confidence intervals for $U(t, \mathbf{r}_j)$. For example, if we choose $p = 95$%, then each annulus has probability 0.95 of containing the true location of the signal. Each annulus is statistically independent, so the intersection of three annuli has probability p^3 of containing the signal's horizontal location. If we want the final region to be valid with a probability of P percent we choose $p = P^{1/3}$. A geometrical interpretation of location is made with the picture of intersecting circles or annuli, the projections of spheres or thick spheres onto a horizontal plane.

4.3. Time Differences of Arrivals (TDOA)

For TDOA data, the procedure for estimating $U(t, \mathbf{r}_j)$ is the same as data for direct-path times. However, when it comes to locating signals in the 2D plane, the problem is different: location cannot be interpreted by intersecting hyperbolas. When the 2D effective speed is not the same value for each section, we have the problem of finding the locus of points in space satisfying,

$$t_1 - t_2 = \frac{l_1}{c1_{\text{flat}}} - \frac{l_2}{c2_{\text{flat}}}. \tag{11}$$

Here, the 2D effective speeds between the object and receivers 1 and 2 are $c1_{\text{flat}}$ and $c2_{\text{flat}}$ respectively. If they are equal, Eq. (11) becomes

$$t_1 - t_2 = \frac{(l_1 - l_2)}{c1_{\text{flat}}}, \tag{12}$$

and multiplying by the denominator yields Eq. (10) defining the hyperbola: the locus of points in space whose difference in distance is constant from two points.

The locus of points in space whose difference in *signal time* is constant is an isodiachron, derived from the Greek words "iso" for same and "diachron" for difference in time [18]. This is a natural geometry for understanding locations when the effective speeds differ, as for this 2D location model. Consider its shape in the ocean where two receivers are on the bottom at depth 4000 m and on the x axis at ±1000 m. The source is nearby horizontally, (−1500, 500), but not vertically, because we set its depth to 15 m. The 3D effective speed is c = 1450 m/s and the 2D effective speeds are derived with Eq. (4): $c1_{\text{flat}}$ = 253.33 m/s and $c2_{\text{flat}}$ = 781.43 m/s respectively. The measured TDOA is 2.7912 − 3.2626 = −0.4714 s. The isodiachron looks like a circle for this case, and it intersects the true location of the source (Fig. 8). The hyperbola is drawn for a difference of distance given by $c(t_1 - t_2) = 1450(-0.4714)$ $m = -683.5$. It does *not* contain the true location (Fig. 8). Isodiachrons do not always look like circles: sometimes they look ellipse-like and other times even more convoluted (i.e. Fig. 1b in [18]). Unlike hyperbolas, they never extend to infinity when the effective speeds differ: a desirable quality of any geometrical interpretation of location [18].

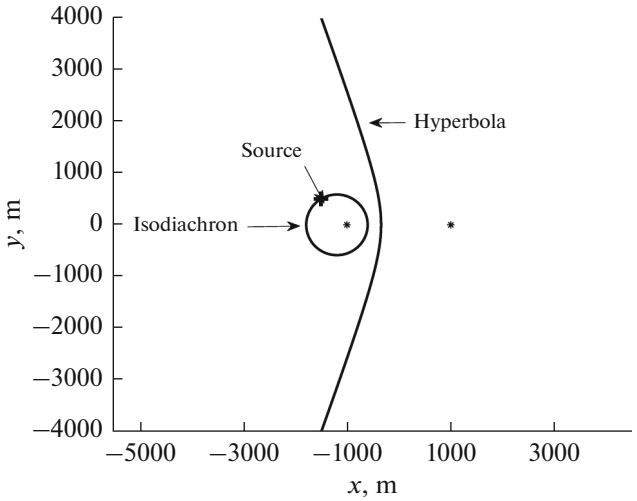

Fig. 8. Geometrical shapes for locating horizontal location of object in ocean with a 2D model from measurements of Time Differences of Arrival at two receivers (asterisks) assuming 2D effective speed is spatially homogeneous (hyperbola) and inhomogeneous (isodiachron). Receivers about 4000 m deeper than source (Sec. 4.3). True horizontal location of source is on isodiachron (+).

Confidence limits for direct-path times were annuli (Sec. 4.2). Isodiachrons do not maintain the same shape as effective speeds change: we cannot zoom them in and out as we did for circles to get confidence intervals. Instead, we could choose many pairs of 2D effective speeds within the desired confidence interval, and draw the isodiachrons for each realization: they will fill a finite region of space, and the realizations can be plotted to show corresponding confidence intervals. Alternatively, confidence intervals could be computed with Sequential Bound Estimation [4, 19], a technique discussed later.

4.4. Vertical Coordinate Constraint for Object

We consider how to estimate a reliable confidence interval for an object's location with prior information of its vertical coordinate. The approach is the same as the previous section except the grid of points, (x_k, y_k, z_k), is constrained to a smaller subset of the vertical coordinate z. For example, suppose we locate a surface ship: we set $z_k = 0$ where the water surface is at zero. If we know a whale is in the upper 100 m, the grid of points only includes values between zero and 100 m depth.

5. RELIABLE CONFIDENCE INTERVALS FOR LOCATION ACCOUNTING FOR ALL ERRORS

The previous section quantified errors in 2D location when the 2D effective speed is constant. These errors go to zero if the 2D effective speed is allowed to vary. This highly idealized scenario was presented to show why variable propagation speed is needed in the simplest situation. The purpose of this section is to show how this effect is incorporated into a model accounting for all significant phenomena affecting location, including refraction, diffraction, multipath, uncertain vertical coordinate of the source, uncertainties in the 3D sound speed field, locations of receivers, and TDOA measurements. The model is appropriate for locating real acoustic signals in air and water.

This realistic model yields extremely reliable confidence intervals. They are computed with a non-Bayesian method called Sequential Bound Estimation (SBE) [4]. It solves the nonlinear equations for location without approximation. Analytical solutions for location are obtained with isodiachrons [18]: we allow the 2D effective speed to differ between sections and have uncertainty along each section. Two sections have probability zero of having the same 2D effective speed. Because isodiachrons do not extend to infinity, we are guaranteed locations are finite [18] as long as we impose finite bounds on all other variables affecting location. The most useful output of SBE is a 100% confidence interval for location. To date, this interval always contains the true answer both in tens of thousands of simulations and experiments having independent measurements for location of the source [20]. 2D effective speed is constrained to a finite-width interval and simulations include deep and shallow water scenarios where sound speed varies horizontally and vertically over a wide variety of bottom profiles. The model was independently tested by the Navy in deep water [20]. The software is at Transition Readiness Level 6 [21].

In this paper, inputs to SBE are 100% intervals for receiver locations, 2D effective speeds between the source and each receiver, and TDOAs between each receiver and receiver number one: all are large enough to contain the true answer. Since there are five receivers, there are four TDOAs. Bounds for the 2D effective speed are computed by first computing bounds for the 3D effective speed. This is done by running numerous ray or full-wave forward-models for the study area and tabulating bounds for the first multipath's arrival time, $[\check{t}, \hat{t}\ ]$. These forward models capture the plausible variations of the sound speed field and the vertical coordinate of the source. Since the forward models specify the distance between the source and receiver for each scenario, we derive bounds for the 3D effective speed by dividing each distance by bounds for arrival time and then converting to bounds for 2D effective speed with Eq. (4). The forward models are done before the experiment starts.

We need to estimate with data the TDOA corresponding to the first arriving path. This is straightforward when there are no multipath. When the signals are coherent enough, cross-correlation is effective. With multipath, cross-correlation is still useful for estimating the needed TDOA as long as it is possible to identify the peak in each cross-correlation function corresponding to the first arrivals. Since the largest peak in a cross-correlation function may not correspond to the first-arriving paths, a method is employed to identify the needed peak using additional information derived from the auto-correlation functions of the signals at each receiver [22]. This method works with data.

Before showing results with SBE, we derive the horizontal locations where a 2D model is valid.

5.1. Valid Locations in 2D Models for Sequential Bound Estimation

Using Eq. (4), the minimum and maximum 2D effective speeds are

$$\check{u} = \frac{\hat{c}}{\sqrt{1 + \dfrac{\hat{v}^2}{\check{h}^2}}}, \tag{13}$$

and

$$\hat{u} = \frac{\check{c}}{\sqrt{1 + \dfrac{\check{v}^2}{\hat{h}^2}}}, \tag{14}$$

respectively. Bounds for the 3D effective speed, $[\check{c}, \hat{c}]$, are computed by a model or some other method: they are guaranteed to contain the true 3D effective speed. Similarly, bounds for the vertical distance between source and any particular receiver are specified with $[\check{v}, \hat{v}]$. Let $\check{h}$ be the minimum horizontal distance of a source from a receiver, by specifying bounds for the 2D effective speed, $[\check{u}, \hat{u}]$. Invalid regions are the set of

points where the horizontal distance is less than $\check{h}$. We set $\hat{h}$ to be the maximum horizontal distance of signal detection. Then we solve for the maximum 2D effective speed $\hat{u}$ from Eq. (14) because all values on its right side are known. We specify the interval width of the 2D effective speeds with

$$\delta u \equiv \hat{u} - \check{u} = f(\hat{c} - \check{c}), \tag{15}$$

where the number f is specified. Larger values of f are associated with wider bounds. Reliable 2D location models yield confidence intervals assuming the 2D effective speed is somewhere within an interval: the larger the interval, the larger the error of location but the closer the source can be to a receiver. This is a natural trade-off. To get $\hat{h}$, we equate δu from Eq. (15) with $\hat{u} - \check{u}$ from Eqs. (13), (14), and solve for the remaining unknown

$$\check{h} = \frac{\hat{v}}{\sqrt{a^2 - 1}}, \tag{16}$$

where

$$a \equiv -\frac{-\check{c}}{\left(\delta u - \dfrac{\hat{c}}{\left(1 + \dfrac{\check{v}^2}{\hat{h}^2}\right)^{1/2}}\right)^{1/2}}. \tag{17}$$

5.2 Example

We assume the acoustic source is between 1 and 100 m depth with a maximum horizontal detection range of $\hat{h} = 15$ km. Receivers are a few hundred meters deeper: between 280 and 300 m depth. They are situated within ±25 m of the vertices of a pentagon (Fig. 9). The bounds of the 3D effective speed are $\check{c} = 1440$ and $\hat{c} = 1455$ m/s. The maximum 2D effective speed is computed from Eq. (14) using the minimum vertical distance between source and receiver: $\check{v} = 280 - 100 = 180$ m: we get $\hat{u} = 1454.90$ m/s.

We specify the interval width for 2D effective speed using $f = 1.2$ in Eq. (17). The minimum 2D effective speed is $\check{u} = 1436.90$ m/s (Eq. 15). Finally, Eq. (16) yields the minimum horizontal distance of any receiver to the first valid location: $\check{h} = 4545.9$ m, an astonishingly large distance for a situation where receivers are only a few hundred meters deeper than the source and where the receivers are separated by many kilometers. Invalid regions are shaded gray (Fig. 9). If we wanted valid results nearer a receiver, we would increase f with attendant increase in the confidence interval for the source's location.

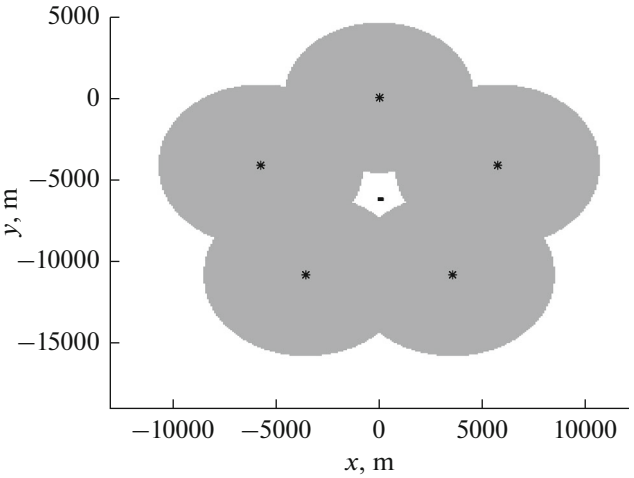

Fig. 9. Extremely reliable 100% confidence interval for source near center (black) computed from TDOAs between signals from five receivers (asterisks). 2D effective speed equals zero at asterisks. Receiver's depths are a few hundred meters below the source (Sec. 5.2). Invalid regions of 2D model are gray. Locations computed with sequential bound estimation and isodiachrons [4, 18].

The significance of utilizing reliable confidence intervals is better understood by realizing $\check{h} = 4545.9$ m is *not* the same as obtained by solving Eq. (4) for h,

$$h = \frac{v}{\sqrt{\left(\dfrac{c}{u}\right)^2 - 1}}, \tag{18}$$

and finding its minimum

$$h \neq \frac{\check{v}}{\sqrt{\left(\dfrac{\hat{c}}{\check{u}}\right)^2 - 1}}, \tag{19}$$

yielding 1130.5 m: smaller than 4545.9 m. The value 1130.5 m is *only* true if the vertical separation is $\check{v} = 180$ m, the maximum 3D effective speed is 1455 m/s, and the minimum 2D effective speed is 1436.9 m/s. If we knew these were the only possible values for the vertical separation and 3D and 2D effective speeds, $\check{h} = 1130.5$ m would be the correct value. However, we do not know the vertical separation, nor the 3D or 2D effective speeds. Instead we are only certain they fall somewhere within their specified intervals. Since we require an extremely reliable confidence interval, we enforce their intervals of prior uncertainty, yielding $\check{h} = 4545.9$.

TDOAs are assumed to be within ±0.02 s of the true TDOAs. SBE yields a 100% confidence interval for the source within the x interval [−66.1, 213] m and the y interval [−6300, −6110] m (small black rectangle,

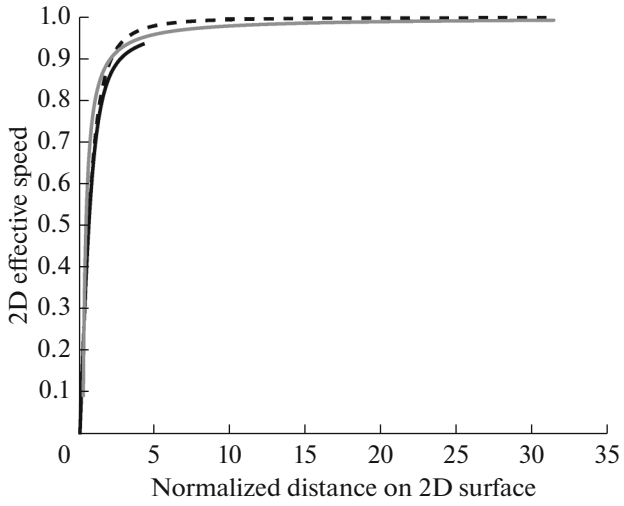

Fig. 10. 2D effective speeds for planar (dashed) and spherical (solid black) 2D models. Planar 2D effective speeds computed with Eq. (4) for 3D effective speed $c = 1$, vertical offset, $v = 0.1$, and horizontal axis showing horizontal distance h from instrument divided by v. Spherical 2D effective speeds computed with Eq. 20 (Sec. 6). Gray curve is functional form for the radial speed of light in Schwarzschild's coordinates for an event horizon of radius 0.01 and a local speed of light equal to one (Sec. 7).

Fig. 9). These contain its true location $x = 49.1$ m and $y = -6210$ m. In this case, SBE identifies the location of the source within the valid regime of the 2D model, and yields its reliable confidence interval. Our reliable location algorithm does not use a 2D SBE model to compute a reliable confidence interval if the source was in an invalid region. Instead it yields a reliable confidence interval with its built-in 3D location model; the hybrid solution discussed in Sec. 3.4.

Invalid regions of the 2D model are close to the instruments, and the valid regions occur far away (Fig. 9). The method for determining where 2D models are valid is applicable at any distance, not just those treated up to 15 km from the instruments (Fig. 9).

6. OTHER FLATLANDS

Up to this point, we discussed 2D models with planar coordinates. Sometimes, horizontal coordinates are desired in latitude and longitude, and the 2D model surface is a sphere or spheroid [10]. We discuss the 2D effective speed for the sphere because it is simpler.

Assume the sphere has radius R and the object to locate is above the sphere at radius $\rho = r + v$ with $v \geq 0$. As before, assume the 3D effective signal speed is c. In the context of the 2D model, signals propagate along great circles of length h on the 2D spherical surface, instead of straight line segments of planar 2D models (Sec. 1). The Euclidean distance between the object and instrument is $d = \left[(\rho\sin\theta)^2 + (R - \rho\cos\theta)^2\right]^{1/2}$, where θ is the angle between two line segments, the first between the sphere's center and the instrument, and the second between the sphere's center and the object. The horizontal distance of the signal path on the sphere is $h = R\theta$. The 2D effective speed for the sphere is obtained by substituting this h and d into Eq. (3),

$$u_{\text{sphere}} = \frac{cR\theta}{\left[2R^2(1-\cos\theta) + 2vR(1-\cos\theta) + v^2\right]^{1/2}}. \quad (20)$$

Although this 2D effective speed goes to zero when h goes to zero, its functional form is not the same as the planar 2D effective speed (Eq. 4). For small horizontal separation, $\cos\theta \sim 1$ and $u_{\text{sphere}} \sim ch/v$: the same form as the planar model to leading order in h (Eq. 4). If we assume the direct path does not propagate through the spherical surface, a signal is received when $|\theta| \leq \cos^{-1} R/\rho$ or $h \leq R\cos^{-1} R/\rho$. The planar and spherical 2D effective speeds differ (Fig. 10). Spherical 2D effective speeds do not exist when $h > R\cos^{-1} R/\rho = 0.43$. Since the figure shows normalized horizontal separation, h/v, values do not exist when $h/v > 0.43/0.1 = 4.3$.

When the 2D model surface is a spheroid [10], there is no closed-form solution for the 2D effective speed because geodesic length h does not have a closed-form expression. Instead, 2D effective speeds are computed with Eq. (4) and h is computed numerically.

7. SUMMARY AND CONCLUSIONS

Signal times have been used for a century to locate signals on 2D surfaces even though objects are not usually on this surface. Their ubiquitous use up to the present suggests correctness of approach [1–6, 9, 13]. However, since it is reasonable to insist correct locations be obtained from any coordinate system, including 2D, we are forced to make the model's speed depend on geodesic length between the object and instrument on the model's 2D surface. 2D effective speeds are zero at the horizontal coordinates of the receivers and monotonically increase to the 3D effective speed at infinite distance (Eq. 4). The apparent discovery here of these facts suggests findings in thousands of papers could be re-evaluated. Many results must be approximately correct, while others must not. Traditional 2D models yield large errors near the instruments. An experimentalist naturally places instruments near signals of interest, thinking errors will be smaller. This is exactly where the 2D model's signal speed goes to zero, leading to large errors with traditional methods and small errors with non-traditional methods (Sec. 5). The traditional 2D model with constant speed is most accurate at distances far from the instruments only when the 2D effective speed equals the 3D effective speed and only in certain azimuthal directions but not in others where its errors increase (Fig. 6a). However, if the 2D effective speed

is slightly different than the 3D effective speed, errors are much larger and occur over a wider sweep of azimuthal directions (Fig. 6b).

Almost all previous 2D models set signal speed to a constant, independent of an object's location. In a small number of cases, 2D models constrain signal speeds to an interval of finite-width [4, 6], and the reported interval does not ever appear to include zero. Furthermore, the interval does not include the significant effect of signal speed varying with distance from instruments. When the signal speed is constrained to an interval, the 2D model can only generate reliable confidence limits for location in certain areas of the 2D surface (Sec. 4). These are called valid regions of the model. The complementary regions are invalid. I presented one approach to delineate the valid and invalid regions of 2D models based on sequential bound estimation and isodiachrons (Sec. 5).

Locations from 2D models can be interpreted geometrically. For direct-path times, geometry is conventional. Locations are visualized by intersecting circles: the projection of a sphere on a flat surface. For TDOA, 2D effective speeds can differ by large factors between the object and each receiver. Location is visualized by intersecting isodiachrons [18]: the replacement for hyperbolas when the propagation speed of the signal is spatially inhomogeneous. Collapsing a 3D problem onto 2D eliminates the spatial homogeneity of signal speed. Geometries are transformed from shapes invented by ancient Greek mathematicians into geometries of the modern age wherein locations are derived with signal times and spatially inhomogeneous speeds [18, 19].

Errors are not discussed in 2D models for bistatic data. Signal times are measured between a source, reflector and a receiver. When they are all on a Euclidean plane, each bistatic measurement of signal time constrains location of the reflector to an ellipse in the absence of measurement error. When the reflector is not in this plane, signal speed must vary with distances from the instruments to obtain a correct location. Locations are obtained with analogous approaches and location can visualized by intersecting isosigmachrons instead of ellipses [23].

It is showed how a variable 2D effective speed is incorporated into a 2D model, and how to switch to a 3D model when the 2D approximation cannot be made valid (Sec. 5). I showed how a combination 2D/3D model can be constructed to yield extremely reliable confidence intervals for location. The model works with real data and accounts for real issues that arise in the air and water such as multipath, inhomogeneities in the speed of sound, refraction, uncertainties in locations of the receivers, and measurements of the TDOA (Sec. 5).

The problems with 2D models are fundamentally related to issues arising in the transformation of coordinate systems. There are five phenomena that arose because of the elimination of the third spatial coordinate. Firstly, locating objects with signal times is simpler in one coordinate frame (3D) than another (2D). Secondly, a method can be used to infer something about a larger dimensional coordinate system through a measurement in the lower dimensional system. For example, we saw how scientists in Flatland inferred the existence of a third spatial dimension of the universe through measurements of signals times on their 2D world (Sec. 2). Thirdly, physics cannot depend on coordinates and correct location and its correct confidence interval must be independent of coordinate-frame. The enforcement of this principle led to the discovery of signal speed varying with distance from an instrument in 2D coordinates (Sec. 2). Fourthly, the speed of a signal varies with distance from an instrument in 2D but not in 3D coordinates. Fifthly, the geometry for interpreting the physics depends on coordinate system. Hyperbolas are the natural geometry in 3D space when signal speed is spatially homogeneous. In the 2D coordinate system, signal speed is spatially inhomogeneous in the extreme, and isodiachrons are a natural geometry for interpreting location. It is interesting to see how similar phenomena occur in special relativity, general relativity (GR), and electromagnetism due to transformation of coordinates.

The five phenomena above are treated in the same order. Firstly, Kaluza sent Einstein a letter in 1919 showing how the addition of a fifth coordinate could simplify physics by unifying electromagnetism and GR (p. 671 in [24]). Secondly, it is possible to determine if space is curved using local measurements. Suppose we live on a 2D surface and wonder if it is a Euclidean plane or a sphere. We can draw a circle on this 2D world and measure the ratio of its circumference to its radius. If the ratio equals 2π, the surface is flat. Otherwise it is curved (p. 6 in [24]). The measurement is made entirely in the 2D world and the existence of something otherwise invisible is revealed. This is like the discovery of a third spatial dimension of the universe by Flatland-scientists (Sec. 2). Thirdly, the findings in special relativity are derived by insisting the speed of light is the same for all coordinate systems moving with uniform velocity [24]. The variation of signal speed in 2D models is derived by insisting correct locations are derived for 2D coordinates. Fourthly, according to GR, the radial speed of light varies with distance from a black hole in Schwarzschild's coordinates but not in local coordinates [25]. This is discussed below. Fifthly, in GR the geometry of spacetime is flat in local coordinate systems but is not-flat in all non-local coordinates such as Schwarzschild's [24]. The appropriate geometry replacing Minkowski spacetime for flat space is Riemannian geometry in non-local coordinates. For 2D models, the new geometry is the isodiachron.

In Schwarzschild's coordinates, the radial speed of light is

$$\frac{dr}{dt} = \left(1 - \frac{r_s}{r}\right)c, \quad (21)$$

where t is time measured by a clock at infinite distance from the black hole, r is zero at its center, $2\pi r_s$ is the circumference of a circle on the event horizon, and c = 299792458 m/s is the speed of light in local coordinates [25]. The decrease in light speed in a gravitational field is experimentally verified, and is known as the Shapiro effect [26]. In local coordinates the speed of light is 299792458 m/s, but in Schwarzschild's coordinates is zero at the event horizon. The physics that causes the radial speed of light to vary from zero to 299792458 m/s is different than the physics that causes the speed of a signal to vary from 0 to the 3D effective speed in 2D models. What is not a coincidence is the role of coordinate transformations in determining how speed varies with location. This is further illuminated by Professor Khoury who developed a coordinate system in GR where the radial speed of light obeys the same functional relationship with distance as the 2D effective speed given by Eq. (4) (version 2 of [23]).

In light of the role of coordinate systems and metrics in describing similar phenomena in 2D models and GR, it makes sense to call locations where the 2D effective speed is zero "2D black holes". The radius of their event horizons equals zero. Similarly, we can refer to invalid regions of 2D models as "2D shadows". They always contain one or more 2D black holes. 2D black holes are not the same as sonic black holes, a phenomenon predicted by Unruh in 1981, where sound has difficulty escaping from a current exceeding the local speed of sound [27]. The 2D shadows are not the shadow zones of caustics encountered in optics and acoustics. The ideas in this theoretical paper need to be evaluated independently with data from past and future experiments. The methods for treating 2D location models are equally applicable to acoustic and electromagnetic signals.

ACKNOWLEDGMENTS

Author thanks Professor J. Khoury at the University of Pennsylvania for discussions concerning gravitational black holes. Author thanks Professors R. Giegengack and M. Putt (University of Pennsylvania) and Dr. E. Terray for their insightful comments. Dr. D. Agnew (University of California San Diego) found [1]—the earliest use he could find of location derived with TDOAs in 2D models. Author thanks the reviewer for their comments. Time for composing this paper was provided by ONR contract N0001417C0230.

REFERENCES

1. J. Milne, *Earthquakes and other Earth movements* (D. Appleton and Co., New York, 1886).
2. H. Bateman, Mon. Weather Rev. **46**, 4 (1918).
3. D. K. Mellinger, *Ishmael 1.0 User's Guide* (NOAA/Pacific Marine Environmental Lab., Seattle, WA, 2001).
4. J. L. Spiesberger, J. Acoust. Soc. Am. **118**, 1790 (2005).
5. T. Dutoit, V. Kandia, and Y. Stylianou, *Applied Signal Processing* (Springer, Boston, MA, 2009), Chap. 6, p. 185.
6. G. A. Warner, S. E. Dosso, and D. E. Hannay, J. Acoust. Soc. Am. **141**, 1921 (2017).
7. W. Hu, M. Fu, and Y. Yang, in *Proc 3rd Int. Conference on Intelligent Human-Machine Systems and Cybernetics* (IEEE *Computer* Society, Los Alamitos, 2011), Vol. 2, p. 19.
8. P. S. Suwal, MSc Thesis (Portland State Univ., Portland, 2012).
9. X. Lou, W. Li, and J. Lin, ISRN Appl. Math. **2012**, 1 (2012).
10. E. A. Lewis, R. B. Harvey, and J. E. Rasmussen, J. Geophys. Res. **65**, 1879 (1960).
11. S. W. Kruger, MSc Thesis (North-West Univ., Potchefstroom, 2017).
12. S. C. Lee, W. R. Lee, and K. H. You, *Communications in Computer and Information Science,* in *Control and Automation*, Ed. by D. Ślęzak, T. Kim, A. Stoica, and B. H. Kang (Springer, Berlin, 2009), **Vol. 65**, p. 35.
13. B. Jin, X. Xu, and T. Zhang, Sensors **18**, 1 (2018).
14. X. Li, Z. D. Deng, L. T. Rauchenstein, and T. J. Carlson, Rev. Sci. Instrum. **87**, 041502 (2016).
15. K. L. Cummins and M. J. Murphy, IEEE Trans. Electromagn. Compat. **51**, 499 (2009).
16. C. Rascon and I. Meza, Rob. Auton. Syst. **96**, 184 (2017).
17. R. O. Schmidt, IEEE Trans. Aerosp. Electron. Syst. **AES-8**, 821 (1972).
18. J. L. Spiesberger, J. Acoust. Soc. Am. **116**, 3168 (2004).
19. J. L. Spiesberger, US Patent No. 7219032 (2007).
20. J. L. Spiesberger, *Final Report. Target Localization Using Multi-Static Sonar with Drifting Sonobuoys, Contract N68335-12-C-0002* (Naval Air Warfare Center).
21. *Defense Acquisition Guidebook* (2013).
22. J. L. Spiesberger, J. Acoust. Soc. Am. **106**, 837 (1999).
23. J. L. Spiesberger (2018). https://arxiv.org/abs/1811.05539.
24. A. Zee, *Einstein Gravity in a Nutshell* (Princeton Univ. Press, Princeton, 2013).
25. J. Branson, *The Singularity in Schwarzschild Coordinates* (2012). https://hepweb.ucsd.edu/ph110b/110b.notes/node77.html.
26. I. I. Shapiro, Phys. Rev. Lett. **13**, 789 (1964).
27. W. G. Unruh, Phys. Rev. Lett. **46**, 1351 (1981)